Limitations of IL-2 and rapamycin in immunotherapy of type 1 diabetes

Baeyens, Audrey ; Pérol, Louis ; Fourcade, Gwladys ; Cagnard, Nicolas ; Carpentier, Wassila ; Woytschak, Janine ; Boyman, Onur ; Hartemann, Agnès ; Piaggio, Eliane

Abstract: Administration of low-dose interleukin-2 (IL-2) alone or combined with rapamycin (RAPA) prevents hyperglycemia in NOD mice. Also, low-dose IL-2 cures recent-onset type 1 diabetes (T1D) in NOD mice, partially by boosting pancreatic regulatory T cells (Treg cells). These approaches are currently being evaluated in humans. Our objective was to study the effect of higher IL-2 doses (250,000-500,000 IU daily) as well as low-dose IL-2 (25,000 IU daily) and RAPA (1 mg/kg daily) (RAPA/IL-2) combination. We show that, despite further boosting of Treg cells, high doses of IL-2 rapidly precipitated T1D in prediabetic female and male mice and increased myeloid cells in the pancreas. Also, we observed that RAPA counteracted IL-2 effects on Treg cells, failed to control IL-2-boosted NK cells, and broke IL-2-induced tolerance in a reversible way. Notably, the RAPA/IL-2 combination failure to cure T1D was associated with an unexpected deleterious effect on glucose homeostasis at multiple levels, including -cell division, glucose tolerance, and liver glucose metabolism. Our data help to understand the therapeutic limitations of IL-2 alone or RAPA/IL-2 combination and could lead to the design of improved therapies for T1D.

DOI: https://doi.org/10.2337/db13-0214

Limitations of IL-2 and rapamycin in immunotherapy of type 1 diabetes

Audrey Baeyens[1,2,3*], Louis Pérol[1,2,3#*], Gwladys Fourcade[1,2,3], Nicolas Cagnard[4], Wassila Carpentier[5], Janine Woytschak[6], Onur Boyman[6,7], Agnès Hartemann[8,9] and Eliane Piaggio[1,2,3#**].

[1]Université Pierre et Marie Curie Univ Paris 06,

[2]Centre National de la Recherche Scientifique, UMR 7211,

[3]Institut National de la Santé et de la Recherche Médicale (INSERM), U 959, Immunology-Immunopathology-Immunotherapy (I3), 75013 Paris, France

[4]INSERM U580 and [5]Bioinformatics Platform, Faculty of Medicine Paris Descartes, Hôpital Necker-Enfants Malades, 75015 Paris, France

[5]Plate-forme Post-Génomique P3S, UPMC Univ Paris 6, Faculty of Medicine, 75013 Paris, France.

[6]Laboratory of Applied Immunobiology, University of Zurich, CH-8006 Zurich, Switzerland.

[7]Allergy Unit, Department of Dermatology, University Hospital Zurich, CH-8091 Zurich, Switzerland.

[8]Department of Endocrinology, Nutrition and Diabetes, Assistance Publique-Hôpitaux de Paris (AP-HP), Pitié-Salpêtrière-Charles Foix Hospital, Paris, France.

[9]Department of Medicine Faculty, Université Pierre et Marie Curie - Paris 6, Paris, France.

* These authors contributed equally to this work

** Corresponding author: eliane.piaggio@yahoo.com

Current address: Institut National de la Santé et de la Recherche Médicale Unité 932, 75005 Paris, France; and Centre de Recherche, Laboratoire d'Immunologie Clinique, Institut Curie,

75005 Paris, France.

Running title: IL-2 and rapamycin in T1D

World count: 3952

Figures: 8

On line Supplementary material: 1 figure and 2 tables

ABSTRACT

Administration of low-dose IL-2 alone or combined with rapamycin (RAPA) *prevents* hyperglycemia in NOD mice. Also, low-dose IL-2 *cures* recent onset type 1 diabetes (T1D) in NOD mice, partially by boosting pancreatic regulatory T cells (T_{reg} cells). These approaches are currently being evaluated in humans. Our objective was to study the effect of higher IL-2 doses (250,000-500,000 IU, daily) as well as low-dose IL-2 (25,000 IU, daily) and RAPA (1mg/kg, daily) (RAPA/IL-2) combination. We show that despite further boosting T_{reg} cells, high doses of IL-2 rapidly precipitated T1D in pre-diabetic female and male mice and increased myeloid cells in the pancreas. Also, we observed that RAPA counteracted IL-2 effects on T_{reg} cells, failed to control IL-2-boosted NK cells and broke IL-2-induced tolerance in a reversible way. Notably, RAPA/IL-2 combination failure to cure T1D was associated to an unexpected deleterious effect on glucose homeostasis at multiple levels, including β-cell division, glucose tolerance and liver glucose metabolism. Our data help understand the therapeutic limitations of IL-2 alone or RAPA/IL-2 combination and could lead to the design of improved therapies for T1D.

INTRODUCTION

In type 1 diabetes (T1D), the immune system destroys the pancreatic ß-cells(1). At clinical onset, around 30 % of ß-cells are still able to produce insulin(2), thus stopping autoimmune destruction at this stage is a promising approach(3). Along the same lines, there is a growing list of Phase I/II clinical trials based on immunomodulation that are currently being conducted in T1D patients(4).

NOD mice, which develop spontaneous T1D, represent an accepted model to test new therapies(5), the gold standard being that treatments that ***cure*** overt hyperglycemia in these mice may be most appropriate for translation into the clinic, as was the case for anti-CD3 Abs(6) which have been tested in patients with promising results(7). In addition, results from our own group showing that low-dose IL-2 can prevent(8) and revert disease in NOD mice(9), have led to the translation of this strategy into clinical trials in T1D patients (clinicaltrials.gov, NCT01353833).

We have shown that in NOD mice, administration of low-dose IL-2 for 5 days induced the remission of new onset T1D by specifically boosting regulatory T cells (T_{reg} cells) in the pancreas without activating pathogenic effector T cells (T_{eff} cells). However, remission was obtained in only 60 % of treated mice and half of them became diabetic again during the following months(9). Consequently, improving IL-2 therapy by optimizing dosing or combining IL-2 with other immunomodulatory drugs, such as rapamycin (RAPA), could be of great importance for the goal of translating this therapy to humans.

RAPA has been used in clinical transplantation for many years(10) and it has been safely administered to T1D patients during islet transplantation(11-12). In mice, RAPA monotherapy can prevent T1D development(13), however, it is unable to induce disease reversal(14). Moreover, RAPA and IL-2 were found to be synergistic for prevention of diabetes in NOD mice(13). Consequently, we decided to test whether RAPA could synergize with short-term IL-2 therapy to reverse T1D and reinforce the development of long-term tolerance.

In this work, we have further studied the mechanisms of action of IL-2 and RAPA alone or in combination in the NOD model of T1D.

RESEARCH DESIGN AND METHODS

Mice

NOD mice were bred in our animal facility under specific pathogen-free conditions in agreement with current European legislation. Protocols were approved by The Ethics Committee in Animal Experiment Charles Darwin, France (number Ce5/2012/021).

IL-2 and RAPA treatment

Mice were treated with daily i.p. injections of 25,000 IU, 250,000 IU or 500,000 IU of recombinant human IL-2 (Proleukin, Novartis, France) for the indicated time. RAPA (Rapamune, Wyeth-Lederle) was administered at 1mg/kg, *per os*, a dose that has been previously reported not to be toxic to pancreatic islets(13-14) and to prevent T1D onset in NOD mice(13). Glycosuria was measured using colorimetric strips (Multistix, Bayer) and blood glucose levels were quantified by a glucometer (Optium Xceed, Abbott).

Spleen, LN and tissue-infiltrating lymphocytes preparation

Spleen and LNs (axillary and brachial) and pancreatic lymph nodes (DLN) were isolated and dissociated in PBS-3% FCS. For pancreas-infiltrating lymphocytes preparation, whole pancreas was digested with collagenase/DNase solution and submitted to Percoll density gradient as described(15-16).

Antibodies and flow cytometry analysis

Anti-CD3, anti-CD4, anti-CD8, anti-CD45.1, anti-ICOS, anti-B220, anti-GITR, anti-Ly6C, anti-Ly6G, anti-CD11b, anti-CD11c, anti-CD19, anti-Gr1, anti-IFN-γ, anti-Ki67, anti-pStat5 (pY694) and streptavidin-labeled with phycoerythrin, allophycocyanin , PerCP, PercP-Cy5.5, V500, APC-H7, PE-Cy7, Alexa Fluor-700, Alexa-647 or biotin, were from BD Biosciences. Anti-CD25, anti-CTLA-4, anti-NKp46 and anti-F4/80 labeled with FITC, PE-Cy7, APC or

eFluor 450 were from eBiosciences. The eFluor 450-anti-Foxp3 staining was performed using the eBioscience kit. For intracellular cytokine staining, cells were re-stimulated with 1µg/ml PMA/0.5µg/ml Ionomycin (Sigma) for 3 h, in the presence of GolgiPlug (1µl/ml) (BD Biosciences). For phospho-STAT-5 staining, DLNs were dissociated, immediately fixed in PBS 1.5% formaldehyde and permeabilized in MeOH., Cells were stained in PBS 0.2% BSA medium containing anti-CD4, anti-CD25, anti-Foxp3 and anti-pSTAT5 mAbs. PE-conjugated NRP-V7/H-2^{K} tetramer containing NRP-V7 peptide (KYNKANVFL) and control PE-conjugated TUM/H-$2^{K,}$ tetramer containing TUM peptide (KYQAVTTTL) were kindly provided by Pere Santamaria. Cells were stained in RPMI 2% medium containing NRP-V7/H-2K or TUM/H-2K at room temperature for 2 h, washed and further stained with anti-CD8 and anti-CD4 antibodies. Cells were acquired on a LSR II (BD Biosciences) and analyzed with FlowJo (Tree Star) software.

Histology

Pancreas were fixed in 10% formalin, embedded in paraffin and cut in 2µm thick sections and stained with hematoxylin/eosin. Insulitis scoring was evaluated microscopically.

For immuno-histology, pancreas were embedded in optimal cutting temperature (OCT) medium, snap-frozen in liquid nitrogen and stored at -80°C until use. Eight µm thick-sections were blocked with PBS 2% BSA, stained with anti-mouse insulin (Sigma) followed by biotinylated anti-mouse IgG1 (Abcam) and APC-labeled streptavidin, PE-labeled anti-CD45.1 and FITC-labeled anti-Ki67 (BD Biosciences) and counterstained with Hoechst (Dako). Proliferating β-cells were defined as $Ki67^{+}$ $Insulin^{+}$ $CD45.1^{-}$ and manually counted. For CD11b staining, FITC-anti-CD11b (BD Biosciences) was used. Images were acquired on a Leica epifluorescence microscope and analyzed with Metavue Software.

Determination of wet weight of organs

Organs were weighed before and after lyophilization overnight at 58°C under vacuum and wet weight was calculated by subtracting initial weight from weight after lyophilization, as described(17).

Glucose/insulin tolerance test (IPGTT/ITT)

Twelve week-old non-diabetic NOD female mice were treated for 5 days with PBS, 25,000 IU IL-2, IL-2, RAPA or 25,000 IU IL-2 plus RAPA and the last administration was performed 2h before the beginning of the IPGTT/ITT. For IPGTTs, a single dose of 2g glucose/kg was injected i.p. after 16 h overnight fast. For ITTs, a single dose of 0.75 IU insulin/kg (Humulin R, Lilly) was injected i.p. after 4h fasting and blood glucose levels were determined.

Sample generation and DNA microarray hybridization and analysis

Twelve week-old non diabetic NOD female mice were treated for 5d with PBS, 25,000 IU IL-2, RAPA or IL-2 plus RAPA. Mice were fasted for 16h before the injection of a glucose bolus (2 g/kg) 2h after the last administration of IL-2 and/or RAPA. Four hours after the glucose challenge, mice were euthanized, perfused with 0.9% NaCl and liver was collected. Tissue was processed (TissueLyser II, Qiagen) and RNA was generated (RNeasy Mini kit, Qiagen). RNA quality was verified in an Agilent Bioanalyzer and measured with a Nanodrop 1000 (Thermo Scientific).

Microarray experiments were performed on Illumina MouseWG-6 BeadChip. Data were Quantile normalized using BeadStudio software. The working lists were created by filtering probes with detection p values <0.05 for all the chips and discarding overlapping probes. Each data set was derived from 3 biologically independent replicate samples. Independent

samples were compared by computing fold ratios and filtered at a 1.5-fold threshold for Venn Diagrams and 1.2-fold threshold for pathway analysis. For pathway analysis, GenBank accession numbers were mapped to the Ingenuity database (IPA, http://www.ingenuity.com) to retrieve relevant biological processes.

Microarray data accession number: E-MEXP-3789

Statistical analyses

Statistical significances were calculated using two-tailed unpaired Student *t*-test with 95% confidence intervals. When sample distribution was not normal (as determined by a D'Agostino and Pearson omnibus normality test), Mann-Whitney-Wilcoxon non-parametric test was used. Survival proportions were calculated using the Kaplan-Meier method and statistical significances were calculated using the Gehan-Breslow-Wilcoxon test. All statistical significances were calculated with GraphPad Prism v5.0 software.

RESULTS

High doses of IL-2 are toxic and can precipitate T1D development:

We have previously shown that 5 doses of 25,000 IU IL-2 could revert new-onset T1D in NOD mice in part by specifically boosting pancreatic T_{reg} cells(9). However, not all treated mice were cured and in some of them the beneficial effects were transient. We reasoned that increasing the dose of IL-2 administered may further increase the frequency of T_{reg} cells and thus improve the treatment efficacy.

We first tested the capacity of higher IL-2 doses to prevent T1D development. We found that daily treatment of NOD mice with 250,000 or 500,000 IU IL-2 (i.e., doses ten- or twenty-fold

higher than the dose shown to prevent T1D(8) could be lethally toxic in a dose-dependent manner in 5 week-old mice (**Figure 1A, upper panel**). In pre-diabetic mice at 12-14 weeks of age, this treatment was less toxic but it dramatically precipitated the onset of diabetes after only a few daily injections and in a dose-dependent manner (**Figure 1A, middle and bottom panels**). At the 250,000 IU IL-2 dose, females were significantly more sensitive than males to IL-2-induced acceleration of diabetes (**Figure 1A, bottom panel**).

IL-2 toxicity is mainly associated with vascular leak syndrome (VLS), which can lead to hypotension, pulmonary edema, liver cell damage, and even death(17). We thus measured organ edema after 5 days of high-dose IL-2 administration (**Figure 1B**). Unlike C57BL/6 mice(18), higher cumulative doses of IL-2 were necessary before VLS became evident in NOD mice. Moreover, we observed gender-dependent differences, with lung edema being most prominent in males and liver edema in females. Brain edema did not develop in either group. Additionally, we measured islet infiltration in these mice and observed that 5 days of high-dose IL-2 administration induced a mild increase of invasive insulitis in males (**Figure 1C**).

The rapid onset of T1D, observed as early as after only 3 days of treatment, was not due to an immediate detrimental effect of IL-2 on glucose homeostasis, as administration of 250,000 IU IL-2 did not induce any apparent alteration in glucose metabolism after a glucose bolus administration 2 hours after the IL-2 injection (**Figure 1D**).

Low-dose IL-2-induced T1D remission was associated with T_{reg} cell activation only in the pancreas, whereas T_{eff}, $CD8^+$ and NK cells were not noticeably affected by this treatment(9). On the contrary, high-dose IL-2 induced systemic effects, including increased cell numbers in secondary lymphoid organs, most significantly in the pancreas draining lymph nodes (DLN) (**Figure 2A**). In the DLN (**Figure 2B**), non-draining lymph nodes (LNs) and spleen (not

shown), significantly higher proportions of NK cells along with lower frequencies of total $CD4^+$ T cells but with increased T_{reg} cell proportions, were observed.

In the islets, high-dose IL-2 effects were more pronounced (**Figure 2B**). Notably, total $CD4^+$ T cells were unchanged but an almost double frequency of T_{reg} cells were seen following IL-2 treatment. Also NK, $CD11c^+$ and $CD11b^+$ cells increased after IL-2 administration. Interestingly, in almost all analyzed organs, T_{reg}, T_{eff}, $CD8^+$, NK, B and $CD11b^+$ cells increased their division after high-dose IL-2 administration, as assessed by quantification of Ki67 expression (**Figure 2C**). In particular, more than 80 % of NK and $CD11b^+$ had cycled in the pancreas. Indeed, by immuno-histology analysis these highly proliferative $CD11b^+$ cells were found interspersed around the islets and surrounding blood vessels (**Figure 3A).** Further phenotypic analysis indicated that two subpopulations among $CD11b^+$ cells increased during IL-2 treatment: $CD11b^+$ $Ly6C^+$ $F4/80^+$ cells, likely representing tissue macrophages, and $CD11b^+$ $Ly6G^+$ cells, likely representing neutrophils(19) (**Figure 3B**).

Detailed analysis of the effects of IL-2 on T_{reg} cells indicated that the cytokine increased the expression of Foxp3 and CD25 in a dose-dependent way, suggesting an enhancement of T_{reg} cell fitness (**Figure 4A**). Similarly, even though the frequency of T_{eff} cells was diminished, their activation was potentiated by IL-2 administration, as indicated by the dose-dependent increase in the fraction of $CD25^+$ T_{eff} and $CD8^+$ T cells, mainly observed in the islets (**Figure 4B**). Moreover, T_{eff}, $CD8^+$ and NK cells showed increased IFN-γ production (**Figure 4C**) during treatment with high-dose IL-2. Additionally, among the expanded $CD8^+$ T cell population, we observed a significant increase in the frequencies of $NRPV7^+$ IGRP-specific autoreactive CD8 T cells(20) in the blood and in the islets of the treated mice (**Figure 4D**).

RAPA partially counteracts the activation of pancreatic Treg cells induced by low-dose IL-2

The immunomodulatory effects of RAPA have been attributed to its capacity to preferentially affect activated T_{eff} cells, while T_{reg} cells are less susceptible to its action(21). Consequently, we hypothesized that the beneficial effect of low-dose IL-2 on T_{reg} cells could synergize with the concomitant elimination of pathogenic T_{eff} cells by RAPA after administration of a RAPA/low-dose IL-2 combination.

We analyzed the effects of combined treatment on lymphoid cells in pre-diabetic NOD females, in which insulitis is already important. Administration for 5 days of RAPA alone, low-dose IL-2 alone, or both drugs combined did not induce major changes in absolute numbers and frequencies of T cells in the spleen, LNs and DLN (data not show). In the pancreas, low-dose IL-2 alone did not modify the frequency of total $CD8^+$ or $CD4^+$ T cells (data not shown). However, it modified the T_{reg}/T_{eff} balance by increasing the percentage of T_{reg} cells (**Figure 5A**), which was associated with increased cell division (**Figure 5B**) and increased expression of Foxp3, CD25, glucocorticoid-induced tumor necrosis factor receptor (GITR), ICOS and cytotoxic-T lymphocyte antigen 4 (CTLA-4) (**Figure 5C**). A similar tendency was observed when low-dose IL-2 was combined with RAPA. Notably, the effect of IL-2 on T_{reg} cell numbers or activation was significantly less pronounced in the presence of RAPA (**Figure 5A-C**).

Finally, we examined the effects of treatment on NK cells in the pancreas and observed that their proportion doubled after 5 days of treatment with low-dose IL-2 alone, with the percentage of proliferating cells increasing from low basal levels up to around 60% after treatment (**Figure 5D-E**). Addition of RAPA to IL-2 treatment did not modify the effect of IL-2 on NK cells.

We discarded that the partial counteraction of IL-2 effects on T_{reg} cells by RAPA was due to interference of the JAK/STAT pathway, as IL-2-mediated STAT5 phosphorylation was not modified by the administration of RAPA in vivo (**Figure 6**).

RAPA inhibits the ability of low-dose IL-2 to revert T1D

To test whether RAPA could reinforce the development of long-term tolerance when combined with IL-2, we treated new onset T1D NOD mice with 25,000 IU (low-dose) IL-2 with or without RAPA. In agreement with our previously reported results (9), low-dose IL-2 treatment induced diabetes remission in 57 % of the mice. However, none of the 12 mice that received the combined treatment was cured (**Figure 7A**). We assessed the effects of treatment on pancreatic T cells from these mice: RAPA/IL-2 combination did not modify the percentage of total $CD8^+$ or $CD4^+$ T cells (not shown) but it significantly increased the frequency of T_{reg} cells (**Figure 7B**). Interestingly, RAPA hampered the IL-2-induced reduction in IFN-γ production by $CD8^+$ T cells infiltrating the pancreas (**Figure 7C**), which we had previously shown to be associated with T1D reversal(9). These results may partially explain why RAPA inhibits the ability of IL-2 to revert disease.

To determine whether RAPA had any effect in mice that had reverted from new-onset T1D after low-dose IL-2 therapy, we administered RAPA to NOD mice 10 days after IL-2-induced disease remission. Surprisingly, RAPA precipitated hyperglycemia in all previously cured mice (**Figure 7D**). Of note, in 2 out of 8 treated mice, RAPA induced irreversible hyperglycemia, but in the other 6 IL-2-treated mice, the hyperglycemia triggered by RAPA was transient. Indeed, after RAPA withdrawal and without further addition of IL-2, mice spontaneously became normoglycemic again until RAPA treatment was resumed, at which point mice reversed to diabetes. In some of these mice, the transient occurrence of diabetes upon adding and removing RAPA could be repeated at least three times, indicating that RAPA can reversibly inhibit the tolerogenic effect of IL-2. We analyzed the temporal effect of RAPA on the pancreatic infiltrate. Intriguingly, T_{reg} cell levels in the pancreas were

significantly lower in mice cured from diabetes with IL-2 but which had become diabetic again after RAPA treatment as compared to mice that did not receive RAPA and a significant parallel increase in these cells was observed in the DLN (**Figure 7E-F**). T_{reg} cells returned to initial levels after RAPA withdrawal and restoration of euglycemia, suggesting that under RAPA treatment the migration pattern of $CD4^+$ T cells may be altered.

The combination IL-2 plus RAPA impairs glucose tolerance:

The rapid reversibility of the effect of RAPA on diabetes led us to evaluate whether RAPA was affecting glucose homeostasis. We measured fasting blood glucose levels and performed glucose tolerance tests in pre-diabetic NOD mice previously treated with IL-2, RAPA or both combined. Low-dose IL-2 treatment did not modify glucose homeostasis (**Figure 8A-B**), in agreement with results obtained with high doses of IL-2 (**Figure 1D**). However, RAPA/IL-2 combination induced elevated fasting blood glucose levels (**Figure 8A**) and also, RAPA and RAPA/IL-2-treated mice displayed highly impaired glucose tolerance (**Figure 8B**). Mechanistically, RAPA-induced glucose intolerance could be due to direct β-cell toxicity or to peripheral insulin resistance; we thus monitored β-cell division and performed insulin tolerance tests **(Figure 8C-D).** Even if neither RAPA nor RAPA/IL-2 treatments visibly modified the response to an exogenous insulin boost, RAPA/IL-2 administration significantly reduced basal β-cell proliferation in vivo.

Finally, to better understand how RAPA alone or combined with IL-2 interfered with glucose homeostasis, we studied by microarray analysis the liver response to a glucose challenge. As depicted (**Figure 8E and Supplementary Figure 1)**, the liver transcriptome signature was highly modified by IL-2 alone (81 genes) or combined with RAPA (40 genes), whereas fewer genes were affected by RAPA alone (16 genes). To retrieve relevant biological processes associated to the different treatments, we analyzed the canonical pathways that were most

significant to our data sets (**Supplementary Table 1)**. RAPA- and IL-2-modified transcripts were associated mainly with metabolic and immune pathways, respectively. Interestingly, RAPA/IL-2 combination modified other pathways than each drug alone, most of them involving metabolic functions. These data further document the complex effects of these drugs beyond immune-modulation and may partially explain the associated detrimental effects on glucose homeostasis.

DISCUSSION

Low-dose IL-2 administration represents one promising approach(9) (clinicaltrials.gov, NCT01353833) among the novel immunotherapies being evaluated in T1D patients(4). We reasoned that we could enhance the efficiency with which IL-2 induces a tolerogenic state in NOD mice(9) by increasing its dose. However, higher IL-2 doses dramatically accelerated disease onset and demonstrated a toxicity that could even be lethal. Interestingly, female NOD mice were significantly more susceptible than males to diabetes induction, correlating with the higher incidence of spontaneous T1D in females mice (70 %) compared to males (30%)(23). Additionally, high-dose IL-2-associated organ edema and insulitis appeared dissimilar in males and females, suggesting that IL-2-related side effects may be sex-dependent in the NOD mice.

T1D appeared in some of the mice treated with high-dose IL-2 despite substantial local and systemic increase in the frequency and activation of T_{reg} cells. Disease occurrence could be explained by the concurrent activation of T_{eff}, NK, B, and $CD8^+$ T cells, all of which have been implicated in T1D development(3; 24). Of note, among $CD8^+$ T cells, islet-specific ones were enriched in the pancreas, potentially contributing to the destruction of the β-cells.

Remarkably, high doses of IL-2 induced a previously unreported yet striking increase in $CD11b^+$ myeloid cells in the pancreas. Historically, macrophages have been regarded as mediators of insulitis(25). However recently, myeloid cells have been associated with T1D resistance and prevention in NOD mice(26-28). The role of different myeloid subpopulations in disease pathogenesis is nevertheless still being largely unknown.

Overall, higher doses of IL-2 resulted in a shift from immune tolerance to overt destructive autoimmunity. In the context of human therapy, these results highlight the need to perform thorough immunomonitoring of the broad effects of IL-2 so as to determine the dose that would uniquely act on T_{reg} cells or other regulatory populations.

The potent immunosuppressive properties of RAPA are associated with its capacity to block cell cycle progression and induce T cell anergy and depletion(29), thus impacting on T-cell differentiation and function. In our model, RAPA specifically dampened IL-2 effect on pancreatic T_{reg} cells. Notably, diabetic animals receiving IL-2/RAPA combination showed higher frequencies of pancreatic T_{reg} cells compared to treatment with IL-2 alone, which nevertheless were associated with inefficient control of IFN-γ production by infiltrating T cells. These T_{reg} cells could originate from the expansion of pre-existing natural T_{reg} cells or from the generation of induced T_{reg} cells from T_{eff} cells, probably favored by the pro-inflammatory environment in the islets(30).

We could not attribute the deleterious impact of IL-2/RAPA combination on T_{reg} cell function to interference of RAPA on IL-2-mediated activation of STAT-5. However, although T_{reg} cells are less dependent for survival on the AKT/mTOR pathway than T_{eff} cells(33), it is possible that RAPA inhibition of this pathway may still affect IL-2 action on T_{reg} cells(34-35).

NK cells have been described as having no role(36) or a pathogenic role in NOD T1D(37). In humans, they have been seen as either potentially harmful(38-39) or regulatory(40-41). Thus, their role in T1D progression is still debated. Human NK cells have been found to be significantly increased upon IL-2 administration(42-43), notably in T1D patients(35). In our model, after IL-2 administration NK cells rapidly expanded in the pancreas following IL-2 administration. Of note, the effect of IL-2 on NK cells was not affected by the addition of RAPA, raising the hypothesis that, in comparison to IL-2 monotherapy, RAPA/IL-2 combination may negatively impact on pancreatic T_{reg} cells, while failing to control IL-2-boosted NK cells. This is reminiscent of the previous observation that punctual ablation of T_{reg} cells in NOD-BDC2.5 TCR-transgenic mice resulted in a fulminant form of diabetes characterized by an initial burst in NK cell function which led to IFN-γ–dependent activation of pathogenic T cell populations(44).

Although our data suggest that the deleterious effects of RAPA in IL-2-treated NOD mice may be related to its action on T_{reg} cell function or trafficking, we also found that a short course of RAPA and IL-2 at low doses significantly impaired glucose homeostasis. There have been some reports of renal transplant patients chronically treated with RAPA becoming at risk of developing new-onset diabetes, associated with abnormal glucose and lipid homeostasis and with reduced insulin sensitivity(45). Furthermore, in rodents, chronic RAPA treatment severely impairs glucose tolerance, affecting hepatic gluconeogenesis(46-47), adipocytes lipid uptake(46), skeletal muscle insulin sensitivity(48) and β-cell homeostasis(46). However, RAPA alone prevents T1D development in NOD mice (13; 49) and has been reported to improve T_{reg} cell suppressive function in T1D patients(12). Here, we demonstrate that RAPA administration even for a short period and at doses 2-5-times lower than those reported in the literature(46-47), impaired glucose tolerance, as previously suggested(14), and modified liver glucose metabolism in the NOD model. Moreover, when

combined with IL-2, the negative effects on glucose metabolism were broadened; also inducing elevated basal blood glucose levels and impairing β-cell proliferation. Interestingly, our results showing that RAPA restored diabetes in NOD mice which had been previously cured of new onset disease by IL-2 treatment evoke RAPA effects counteracting anti-CD3 treatment in NOD mice(14).

Recently, a clinical trial testing RAPA/IL-2 combined therapy in new onset T1D patients was halted due to a transient drop in C-peptide levels in all patients, despite effective T_{reg} cell induction(35). Our results showing that RAPA breaks IL-2-induced tolerance and that, in combination with IL-2 it induces glucose intolerance; help understand the inefficacy and deleterious consequences of the combined treatment in T1D. However, RAPA/IL-2 combination can be efficient at boosting T_{reg} cells and inducing tolerance in graft-versus-host disease(42; 50). The latter results, which were observed in hosts devoid of the metabolic alterations associated with T1D, demonstrate the different potential outcomes of the combined treatment depending on the underlying pathology. And even when referring to T1D, it is surprising to observe that RAPA and IL-2 combination can have a completely different outcome in preventive or curative schedules in the NOD mice(13). Probably, in pre-diabetic mice, the effects of RAPA are not strong enough to cause hyperglycemia because, at odds with already diabetic mice, there are enough healthy islets to compensate for the negative effects of RAPA, at least for a short-term treatment.

Our results, together with the accumulated experience in the use of IL-2 and RAPA in the context of T1D prevention or reversal (see recapitulation in Supplementary Table 2), help define the limitations of the application of these drugs in T1D and may contribute to the design of improved IL-2-based therapy**.**

ACKNOWLEDGMENTS

This work was supported by the Agence Nationale de la Recherche (ANR-09-GENO-006-01), EFSD/JDRF/NN 2011 and Inserm/ DGOS 2011 (all to E.P.), and by a FAN grant of University of Zurich (to O.B.).

We are grateful to Pere Santamaria, University of Calgary, Canada for kindly providing us with the NRP-V7 and TUM tetramers and to Benoit Salomon, Inserm U959, Paris; Olivier Boyer, Inserm U905, Rouen and José Cohen, Inserm U855, Créteil for constructive and critical reading of the manuscript. We specially thank Bertrand Blondeau, UMRS 872, Paris, for his valuable advice and technical help and Pedro Carranza supported by CODDIM Ile-de-France, Inserm U959, Paris and Hanem Sadek, Inserm U959, Paris; for technical help. We thank Christelle Enond, Flora Issert, François Bodin, and Serban Morosan, all from the Centre d'Exploration Fonctionnelle, UPMC, for taking good care of the mice. A.B. and L.P. were supported by the Ministère de la Recherche.

Author's contribution: A.B., L.P., G.F., J.W., O.B. and E.P. designed and performed the experiments and analyzed data. N.C and W.C. performed and analyzed microarray experiments. E.P. conceived the project. E.P., A.B. and L.P. wrote the paper. A.H. and all the authors discussed the results and commented on the manuscript.

E.P. is inventor of a patent application related to the use of low-dose IL-2 owned by her public institutions. There is no other conflict of interest.

E.P. is the guarantor of this work and, as such, had full access to all the data in the study and takes responsibility for the integrity of the data and the accuracy of the data analysis

REFERENCES

1. Bach JF: Insulin-dependent diabetes mellitus as an autoimmune disease. *Endocr Rev* 15:516-542, 1994

2. Sreenan S, Pick AJ, Levisetti M, Baldwin AC, Pugh W, Polonsky KS: Increased beta-cell proliferation and reduced mass before diabetes onset in the nonobese diabetic mouse. *Diabetes* 48:989-996, 1999

3. Bluestone JA, Herold K, Eisenbarth G: Genetics, pathogenesis and clinical interventions in type 1 diabetes. *Nature* 464:1293-1300, 2010

4. Waldron-Lynch F, Herold KC: Immunomodulatory therapy to preserve pancreatic beta-cell function in type 1 diabetes. *Nat Rev Drug Discov* 10:439-452, 2011

5. Atkinson MA, Leiter EH: The NOD mouse model of type 1 diabetes: as good as it gets? *Nat Med* 5:601-604, 1999

6. Chatenoud L, Thervet E, Primo J, Bach JF: Anti-CD3 antibody induces long-term remission of overt autoimmunity in nonobese diabetic mice. *Proc Natl Acad Sci U S A* 91:123-127, 1994

7. Bach JF: Anti-CD3 antibodies for type 1 diabetes: beyond expectations. *Lancet* 378:459-460, 2011

8. Tang Q, Adams JY, Penaranda C, Melli K, Piaggio E, Sgouroudis E, Piccirillo CA, Salomon BL, Bluestone JA: Central role of defective interleukin-2 production in the triggering of islet autoimmune destruction. *Immunity* 28:687-697, 2008

9. Grinberg-Bleyer Y, Baeyens A, You S, Elhage R, Fourcade G, Gregoire S, Cagnard N, Carpentier W, Tang Q, Bluestone J, Chatenoud L, Klatzmann D, Salomon BL, Piaggio E: IL-2 reverses established type 1 diabetes in NOD mice by a local effect on pancreatic regulatory T cells. *J Exp Med* 207:1871-1878, 2010

10. Abraham RT, Wiederrecht GJ: Immunopharmacology of rapamycin. *Annu Rev Immunol* 14:483-510, 1996

11. Piemonti L, Maffi P, Monti L, Lampasona V, Perseghin G, Magistretti P, Secchi A, Bonifacio E: Beta cell function during rapamycin monotherapy in long-term type 1 diabetes. *Diabetologia* 54:433-439, 2011

12. Monti P, Scirpoli M, Maffi P, Piemonti L, Secchi A, Bonifacio E, Roncarolo MG, Battaglia M: Rapamycin monotherapy in patients with type 1 diabetes modifies CD4+CD25+FOXP3+ regulatory T-cells. *Diabetes* 57:2341-2347, 2008

13. Rabinovitch A, Suarez-Pinzon WL, Shapiro AM, Rajotte RV, Power R: Combination therapy with sirolimus and interleukin-2 prevents spontaneous and recurrent autoimmune diabetes in NOD mice. *Diabetes* 51:638-645, 2002

14. Valle A, Jofra T, Stabilini A, Atkinson M, Roncarolo MG, Battaglia M: Rapamycin prevents and breaks the anti-CD3-induced tolerance in NOD mice. *Diabetes* 58:875-881, 2009

15. Cassan C, Piaggio E, Zappulla JP, Mars LT, Couturier N, Bucciarelli F, Desbois S, Bauer J, Gonzalez-Dunia D, Liblau RS: Pertussis toxin reduces the number of splenic Foxp3+ regulatory T cells. *J Immunol* 177:1552-1560, 2006

16. Grinberg-Bleyer Y, Saadoun D, Baeyens A, Billiard F, Goldstein JD, Gregoire S, Martin GH, Elhage R, Derian N, Carpentier W, Marodon G, Klatzmann D, Piaggio E, Salomon BL: Pathogenic T cells have a paradoxical protective effect in murine autoimmune diabetes by boosting Tregs. *J Clin Invest* 120:4558-4568, 2010

17. Krieg C, Letourneau S, Pantaleo G, Boyman O: Improved IL-2 immunotherapy by selective stimulation of IL-2 receptors on lymphocytes and endothelial cells. *Proc Natl Acad Sci U S A* 107:11906-11911, 2010

18. Krieg C, Letourneau S, Pantaleo G, Boyman O: Improved IL-2 immunotherapy by selective stimulation of IL-2 receptors on lymphocytes and endothelial cells. *Proc Natl Acad Sci U S A* 107:11906-11911, 2010

19. Fu W, Wojtkiewicz G, Weissleder R, Benoist C, Mathis D: Early window of diabetes determinism in NOD mice, dependent on the complement receptor CRIg, identified by noninvasive imaging. *Nat Immunol* 13:361-368, 2012

20. Trudeau JD, Kelly-Smith C, Verchere CB, Elliott JF, Dutz JP, Finegood DT, Santamaria P, Tan R: Prediction of spontaneous autoimmune diabetes in NOD mice by quantification of autoreactive T cells in peripheral blood. *J Clin Invest* 111:217-223, 2003

21. Battaglia M, Stabilini A, Roncarolo MG: Rapamycin selectively expands CD4+CD25+FoxP3+ regulatory T cells. *Blood* 105:4743-4748, 2005

22. Keymeulen B, Walter M, Mathieu C, Kaufman L, Gorus F, Hilbrands R, Vandemeulebroucke E, Van de Velde U, Crenier L, De Block C, Candon S, Waldmann H, Ziegler AG, Chatenoud L, Pipeleers D: Four-year metabolic outcome of a randomised controlled CD3-antibody trial in recent-onset type 1 diabetic patients depends on their age and baseline residual beta cell mass. *Diabetologia* 53:614-623, 2010

23. Billiard F, Litvinova E, Saadoun D, Djelti F, Klatzmann D, Cohen JL, Marodon G, Salomon BL: Regulatory and effector T cell activation levels are prime determinants of in vivo immune regulation. *J Immunol* 177:2167-2174, 2006

24. van Belle TL, Coppieters KT, von Herrath MG: Type 1 diabetes: etiology, immunology, and therapeutic strategies. *Physiol Rev* 91:79-118, 2011

25. Jansen A, Homo-Delarche F, Hooijkaas H, Leenen PJ, Dardenne M, Drexhage HA: Immunohistochemical characterization of monocytes-macrophages and dendritic cells involved in the initiation of the insulitis and beta-cell destruction in NOD mice. *Diabetes* 43:667-675, 1994

26. Hu C, Du W, Zhang X, Wong FS, Wen L: The role of Gr1+ cells after anti-CD20 treatment in type 1 diabetes in nonobese diabetic mice. *J Immunol* 188:294-301, 2012

27. Fu W, Wojtkiewicz G, Weissleder R, Benoist C, Mathis D: Early window of diabetes determinism in NOD mice, dependent on the complement receptor CRIg, identified by noninvasive imaging. *Nat Immunol* 13:361-368, 2012

28. Yin B, Ma G, Yen CY, Zhou Z, Wang GX, Divino CM, Casares S, Chen SH, Yang WC, Pan PY: Myeloid-derived suppressor cells prevent type 1 diabetes in murine models. *J Immunol* 185:5828-5834, 2010

29. Thomson AW, Turnquist HR, Raimondi G: Immunoregulatory functions of mTOR inhibition. *Nat Rev Immunol* 9:324-337, 2009

30. Battaglia M, Stabilini A, Draghici E, Migliavacca B, Gregori S, Bonifacio E, Roncarolo MG: Induction of Tolerance in Type 1 Diabetes via Both CD4+CD25+ T Regulatory Cells and T Regulatory Type 1 Cells. *Diabetes* 55:1571-1580, 2006

31. D'Alise AM, Ergun A, Hill JA, Mathis D, Benoist C: A cluster of coregulated genes determines TGF-beta-induced regulatory T-cell (Treg) dysfunction in NOD mice. *Proc Natl Acad Sci U S A* 108:8737-8742, 2011

32. Haxhinasto S, Mathis D, Benoist C: The AKT-mTOR axis regulates de novo differentiation of CD4+Foxp3+ cells. *J Exp Med* 205:565-574, 2008

33. Delgoffe GM, Kole TP, Zheng Y, Zarek PE, Matthews KL, Xiao B, Worley PF, Kozma SC, Powell JD: The mTOR kinase differentially regulates effector and regulatory T cell lineage commitment. *Immunity* 30:832-844, 2009

34. Kuo CJ, Chung J, Fiorentino DF, Flanagan WM, Blenis J, Crabtree GR: Rapamycin selectively inhibits interleukin-2 activation of p70 S6 kinase. *Nature* 358:70-73, 1992

35. Long SA, Rieck M, Sanda S, Bollyky JB, Samuels PL, Goland R, Ahmann A, Rabinovitch A, Aggarwal S, Phippard D, Turka LA, Ehlers MR, Bianchine PJ, Boyle KD, Adah SA, Bluestone JA, Buckner JH, Greenbaum CJ: Rapamycin/IL-2 Combination Therapy

in Patients With Type 1 Diabetes Augments Tregs yet Transiently Impairs beta-Cell Function. *Diabetes* 61:2340-2348, 2012

36. Beilke JN, Meagher CT, Hosiawa K, Champsaur M, Bluestone JA, Lanier LL: NK cells are not required for spontaneous autoimmune diabetes in NOD mice. *PLoS One* 7:e36011, 2012

37. Gur C, Porgador A, Elboim M, Gazit R, Mizrahi S, Stern-Ginossar N, Achdout H, Ghadially H, Dor Y, Nir T, Doviner V, Hershkovitz O, Mendelson M, Naparstek Y, Mandelboim O: The activating receptor NKp46 is essential for the development of type 1 diabetes. *Nat Immunol* 11:121-128, 2010

38. Gur C, Enk J, Kassem SA, Suissa Y, Magenheim J, Stolovich-Rain M, Nir T, Achdout H, Glaser B, Shapiro J, Naparstek Y, Porgador A, Dor Y, Mandelboim O: Recognition and killing of human and murine pancreatic beta cells by the NK receptor NKp46. *J Immunol* 187:3096-3103, 2011

39. Schleinitz N, Vely F, Harle JR, Vivier E: Natural killer cells in human autoimmune diseases. *Immunology* 131:451-458, 2010

40. Li Z, Lim WK, Mahesh SP, Liu B, Nussenblatt RB: Cutting edge: in vivo blockade of human IL-2 receptor induces expansion of CD56(bright) regulatory NK cells in patients with active uveitis. *J Immunol* 174:5187-5191, 2005

41. Bielekova B, Catalfamo M, Reichert-Scrivner S, Packer A, Cerna M, Waldmann TA, McFarland H, Henkart PA, Martin R: Regulatory CD56(bright) natural killer cells mediate immunomodulatory effects of IL-2Ralpha-targeted therapy (daclizumab) in multiple sclerosis. *Proc Natl Acad Sci U S A* 103:5941-5946, 2006

42. Koreth J, Matsuoka K, Kim HT, McDonough SM, Bindra B, Alyea EP, 3rd, Armand P, Cutler C, Ho VT, Treister NS, Bienfang DC, Prasad S, Tzachanis D, Joyce RM, Avigan DE,

Antin JH, Ritz J, Soiffer RJ: Interleukin-2 and regulatory T cells in graft-versus-host disease. *N Engl J Med* 365:2055-2066, 2011

43. Saadoun D, Rosenzwajg M, Joly F, Six A, Carrat F, Thibault V, Sene D, Cacoub P, Klatzmann D: Regulatory T-cell responses to low-dose interleukin-2 in HCV-induced vasculitis. *N Engl J Med* 365:2067-2077, 2011

44. Feuerer M, Shen Y, Littman DR, Benoist C, Mathis D: How punctual ablation of regulatory T cells unleashes an autoimmune lesion within the pancreatic islets. *Immunity* 31:654-664, 2009

45. Johnston O, Rose CL, Webster AC, Gill JS: Sirolimus is associated with new-onset diabetes in kidney transplant recipients. *J Am Soc Nephrol* 19:1411-1418, 2008

46. Houde VP, Brule S, Festuccia WT, Blanchard PG, Bellmann K, Deshaies Y, Marette A: Chronic rapamycin treatment causes glucose intolerance and hyperlipidemia by upregulating hepatic gluconeogenesis and impairing lipid deposition in adipose tissue. *Diabetes* 59:1338-1348, 2010

47. Lamming DW, Ye L, Katajisto P, Goncalves MD, Saitoh M, Stevens DM, Davis JG, Salmon AB, Richardson A, Ahima RS, Guertin DA, Sabatini DM, Baur JA: Rapamycin-induced insulin resistance is mediated by mTORC2 loss and uncoupled from longevity. *Science* 335:1638-1643, 2012

48. Cunningham JT, Rodgers JT, Arlow DH, Vazquez F, Mootha VK, Puigserver P: mTOR controls mitochondrial oxidative function through a YY1-PGC-1alpha transcriptional complex. *Nature* 450:736-740, 2007

49. Baeder WL, Sredy J, Sehgal SN, Chang JY, Adams LM: Rapamycin prevents the onset of insulin-dependent diabetes mellitus (IDDM) in NOD mice. *Clin Exp Immunol* 89:174-178, 1992

50. Shin HJ, Baker J, Leveson-Gower DB, Smith AT, Sega EI, Negrin RS: Rapamycin and IL-2 reduce lethal acute graft-versus-host disease associated with increased expansion of donor type CD4+CD25+Foxp3+ regulatory T cells. *Blood* 118:2342-2350, 2011

FIGURE LEGENDS

Figure 1. Administration of high doses of IL-2 to NOD mice: toxicity and diabetes development. (A) Male and female NOD mice of 5 weeks of age (upper panel) or 12-14 weeks of age (middle and bottom panels) were injected daily with PBS (black circles = females; white circles = males), 250,000 IU IL-2 (black squares = females; white squares = males) or 500,000 IU IL-2 (black triangles = females; white triangles = males) during 20 days. Shown are Kaplan-Meier survival curves of treated mice (upper and middle panels) and percentage of diabetes free mice; * $P < 0.05$ (Gehan-Breslow-Wilcoxon test) (bottom panel). (B-C) Male and female NOD mice of 12-14 weeks of age were injected for 5 days with PBS (black circles = females; white circles = males,) or 250,000 IU IL-2 (black squares = females; white squares = males) and analyzed 2 h after the last injection. (B) Wet weight of lung (left panel), liver (middle panel) and CNS (right panel) were determined. Symbols represent individual mice and horizontal lines represent the median. ** $P < 0.01$ (unpaired, two-tailed Student's *t* test). (C) Histological quantification of islet infiltration by immune cells in female and male NOD mice. Shown are percentages of islets with no infiltration (0), peri-insulitis (1), moderate insulitis with less than 50% islet area infiltrated by immune cells (2), and severe insulitis with more than 50% islets area infiltrated by immune cells (3). Pictures show representative islets corresponding to the insulitis score used for analysis. (D) Pre-diabetic female NOD mice of 12-16 weeks of age were fasted for 4 h and injected with PBS or

250,000 IU IL-2 followed by a glucose bolus 2 h later. Results are presented as blood glucose levels during the 4 h follow-up (left panel) and as area under the blood glucose curve (AUC) during the follow-up period (right panel), symbols represent individual mice and horizontal lines represent the median. Data cumulate 2 (A, top panel) to 5 (A, middle and bottom panels) independent experiments or are representative of 1 (B,C) to 3 (D) independent experiments.

Figure 2. Administration of high doses of IL-2 to NOD mice: effects on immune cells. Pre-diabetic female NOD mice of 12-14 weeks of age were treated daily with PBS, 250,000 or 500,000 IU IL-2 during 5 days and analyzed 2 h after the last injection. (A) Absolute cell numbers in DLN, non-draining LNs (LNs) and spleen. (B) Percentage of total $CD4^+$, $CD8^+$, $NKp46^+$ $CD3^-$ (NK), B, $CD11c^+$ and myeloid $CD11b^+$ cells in DLN (upper panel) or in pancreas (lower panel). Right panels indicate the percentage of T_{reg} cells among total $CD4^+$ T cells. (C) Representative histograms of Ki67 expression (left panels) and percentages of $Ki67^+$ cells among indicated populations (right panels) in the DLN and pancreas. Similar results were obtained in male NOD mice (not shown). Data cumulate 3 to 5 independent experiments with 4 to 14 mice per group. Symbols represent individual mice and horizontal lines represent the median. * $P < 0.05$; ** $P < 0.01$; *** $P < 0.001$ (unpaired, two-tailed Student's *t* test).

Figure 3. Administration of high doses of IL-2 to NOD mice: effects on myeloid cells. Mice were treated as in Figure 2. (A) Representative immunofluorescence of cryosections from the pancreas of mice treated with PBS (top) or 250,000 IU IL-2 (bottom), stained with anti-CD11b Abs (green) and Hoechst (blue) (magnification x200). Dashed line indicates blood vessels. (B) Myeloid cell gating strategy: islet infiltrating cells were pre-gated as $CD45^+$ $NKp46^-$ and expression of CD11b versus Ly6C was used to define gates R1 and R2 as shown. Cells in these gates were further analyzed for the expression of F4/80 and Ly6G. Cells

in gate R1 were mostly F4/80$^-$ and Ly6G$^+$, probably representing neutrophils and cells in gate R2 were mostly F4/80$^+$ and Ly6G$^-$, probably representing tissue macrophages. (C) Percentages of cells in gate R1 (upper panel) and R2 (lower panel) in islets, DLN, LNs and spleen of mice in indicated treatment groups. Data cumulate 2 independent experiments with 2 to 5 mice per condition, except for panel A, which is from one experiment with 3 mice per group. Symbols represent individual mice and horizontal lines represent the median. * $P <$ 0.05; ** $P < 0.01$; ***$P < 0.001$ (unpaired, two-tailed Student's *t* test).

Figure 4. Administration of high doses of IL-2 to NOD mice: effects on cell activation and cytokine production. Mice were treated as in Figure 2 and DLN and pancreas infiltrating cells were analyzed by flow cytometry. (A) Left panels: representative contour plots of Foxp3 and CD25 expression in CD4$^+$ T cells in indicated groups. Right panels: relative MFI (mean fluorescence intensity) of Foxp3 and CD25 in T_{reg} cells expressed as relative percentage of the MFI value in non-draining LN of PBS treated mice, which was assigned an arbitrary value of 100%. (B) Percentages of CD25$^+$ cells among CD4$^+$ Foxp3$^-$ (T_{eff} cells) (top) and CD8$^+$ T cells (bottom). (C) Representative contour plots of IFN-γ staining (left panels) and percentage of IFN-γ secreting cells (right panels) among islet-infiltrating CD4$^+$ Foxp3$^-$ (top panels), CD8$^+$ (middle panels) and NK cells (bottom panels) quantified after ex vivo stimulation with PMA-ionomycin. Data are cumulative of 2 to 3 independent experiments with 4 to 9 mice per group. * $P < 0.05$; ** $P < 0.01$; *** $P < 0.001$ (unpaired, two-tailed Student's *t* test). (D) Upper panels: representative histograms of control TUM and NRP-V7 tretramer expression on CD8$^+$ T cells from blood and islets. Lower panels: percentage of NRP-V7$^+$ CD8$^+$ T cells among total CD8$^+$ T cells in blood (left) and in the pancreatic islets (left). Data are from one experiment, symbols represent individual mice and horizontal lines represent the median. * P < 0.05; (unpaired, two-tailed Mann-Whitney test).

Figure 5. Effects of combined low-dose IL-2 and RAPA on immune cells. Pre-diabetic female NOD mice of 12-14 weeks of age were treated daily with PBS (n=10), 25,000 IU IL-2 (n=8), RAPA (1 mg/kg) (n=12) or both (n=10) during 5 days and pancreas-infiltrating cells were collected and stained for flow cytometry analysis 2 h after the last treatment. (A) Percentages of T_{reg} cells among $CD4^+$ T cells. (B) Representative overlay histograms of Ki67 expression (left panel) and percentages of $Ki67^+$ T_{reg} cells (right panel) in indicated groups. (C) Representative overlay histograms of Foxp3, CD25, GITR, ICOS and CTLA-4 expression in T_{reg} cells (upper panels) and respective MFI (lower panels) expressed as relative percentage of the MFI value in non draining LN of untreated mice which was assigned an arbitrary value of 100%. (D) Percentages of $NKp46^+$ $CD3^-$ NK cells among pancreas infiltrating cells. (D) Representative overlay histograms of Ki67 expression (left panel) and percentages of $Ki67^+$ NK cells (right panel). Data are cumulative of 4 independent experiments, symbols represent individual mice, and horizontal lines represent the median. * $P < 0.05$; ** $P < 0.01$; *** $P < 0.001$ (unpaired, two-tailed Student's *t* test).

Figure 6. IL-2 and RAPA effects on STAT5 phosphorylation. Pre-diabetic female NOD mice of 12-16 weeks of age were injected with PBS (PBS), 1 mg/kg RAPA 16 and 2 h before analysis, 250,000 IU IL-2 (IL-2) 2 h before the analysis or the combined treatment (IL-2 + RAPA). Phosphorylation of STAT5 on T_{reg} cells ($CD4^+$ $Foxp3^+$ T cells) and T_{eff} cells ($CD4^+$ $Foxp3^-$ T cells) was determined by flow cytometry. Shown are: the gating strategy to define the percentage of p-$STAT5^+$ Treg and T_{eff} cells (upper graph) and the percentage of p-$STAT5^+$ T_{reg} cells (bottom left panel) or T_{eff} cells (bottom right panel) in the DLN**.** Data are cumulative of 3 independent experiments, symbols represent individual mice and horizontal lines represent the median. *** $P < 0.001$ (unpaired, two-tailed Student's *t* test).

Figure 7: RAPA abrogates IL-2-induced tolerance. New-onset diabetic NOD mice were treated daily for 5 d with PBS or 25,000 IU IL-2, or for 10 d with 1mg/kg RAPA along with 25,000 IU IL-2. (A) Percentage of T1D remission. (B-C) Islet infiltrating cells were analyzed 2h after the last injection. (B) Percentage of T_{reg} cells among $CD4^+$ T cells. (C) Percentage of IFN-γ^+ cells among $CD8^+$ T cells quantified after ex vivo re-stimulation with PMA-ionomycin. Symbols represent individual mice and horizontal bars are mean values. * $P < 0.05$; ** $P < 0.01$; *** $P < 0.001$ (unpaired, two-tailed Student's t test). (D) New-onset diabetic NOD mice were cured by low-dose IL-2 and were treated with RAPA (1mg/kg) 10 days after remission until the appearance of hyperglycemia (for 4 and up to 8 days). Arrows indicate RAPA administration. For some mice in which blood glucose levels normalized after RAPA withdrawal, a subsequent RAPA treatment was initiated after 10 days of normoglycemia, and depending on the individual mice, this cycle could be repeated up to 3 times. Response to treatment of 3 individual mice is shown. "Diabetic" indicates blood glucose levels above 250 mg/dl or positive glycosuria and "Non diabetic" indicates blood glucose levels below 250 mg/dl or negative glycosuria. (E-F) The percentage of $CD4^+$ $Foxp3^+$ T cells among $CD4^+$ cells was analyzed by flow cytometry in the DLN and the islets of individual mice at different points during treatment. (E) Representative dot plots of Foxp3 and CD4 staining among $CD4^+$ T cells. (F) Percentage of T_{reg} cells among $CD4^+$ T cells in the DLN (upper panel) and in the islets (lower panel). Symbols represent individual mice and horizontal lines represent the median. Cured= IL-2 cured mice (n=6); diabetic after RAPA= mice that became diabetic under RAPA treatment (n=5); reverted after RAPA withdrawal= mice that regained normal glucose homeostasis after RAPA withdrawal (n=3). * $P < 0.05$ (unpaired, two-tailed Mann-Whitney test).

Figure 8. A short course of RAPA alone or combined with IL-2 induces glucose intolerance. Pre-diabetic female NOD mice were treated for 5 days with PBS, 25,000 IU IL-2, 1 mg/kg RAPA, or IL-2 and RAPA combined. (A-B, E) On day 5, an intra-peritoneal glucose tolerance test (IPGTT) was performed after an overnight fast or mice were euthanized 4 h after the glucose bolus for transcriptome analysis of the liver. (A) Fasting blood glucose levels were determined before glucose injection. (B) Shown are blood glucose levels and area under the blood glucose curve (AUC) of the treated mice of the different groups (n=7-8 per group). Data are cumulative of 2 independent experiments with 7 mice per group. Symbols represent individual mice and horizontal lines represent the median. * $P < 0.05$; ** $P < 0.01$; *** $P < 0.001$ (unpaired, two-tailed Student's t test). (D) Percentage of $Ki67^+$ cells among total beta cells ($insulin^+$ $CD45.1^-$). Each column represents the mean ± SEM of all islets counted for all mice of the same group (n=3-4 per group). * $P < 0.05$ (Mann-Whitney test). (D) On day 5, an insulin tolerance test (ITT) was performed after a 4 h fast. Shown are blood glucose levels and area under the blood glucose curve (AUC) of the treated mice of the different groups (n=7 per group). Symbols represent individual mice and horizontal lines represent the median. (E) Venn diagram comparing differentially expressed genes in the liver after glucose challenge of mice in IL-2 vs. PBS, IL-2/RAPA vs. PBS and RAPA vs. PBS groups. The threshold for differential expression was defined as 1.5-fold changes in expression with overlapping probes discarded. Each number represents the number of genes in each subgroup: total number of genes (Total) and up-regulated (Up, or U) and down-regulated (Down, or D) probes from reference PBS. Each data set was derived from 3 biologically independent replicate samples.

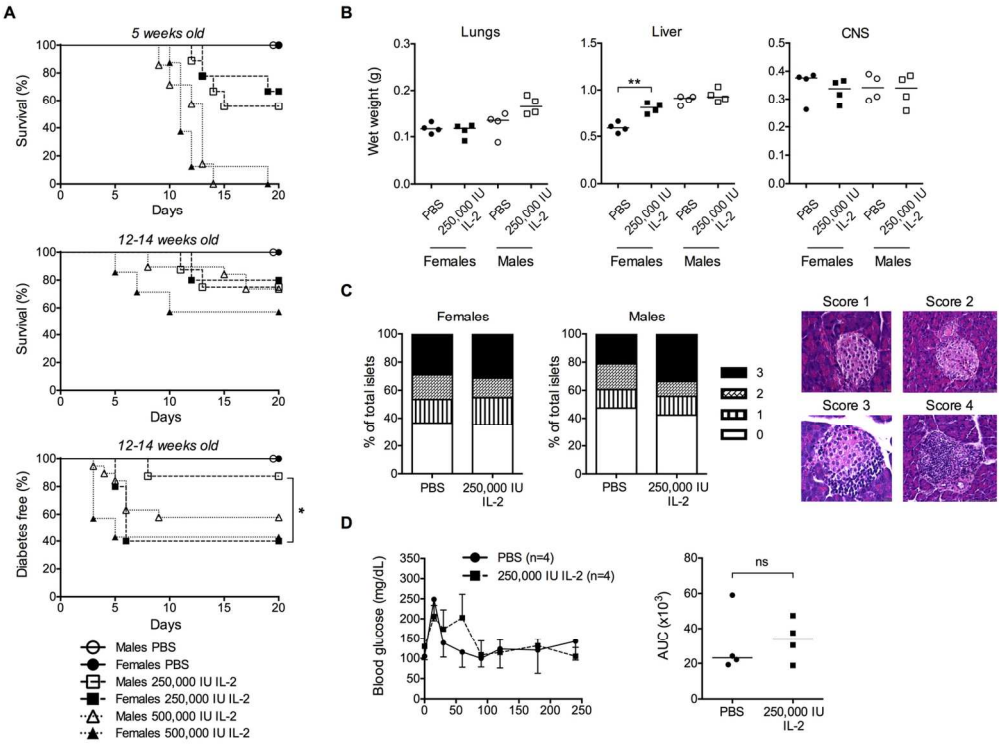

Figure 1. Administration of high doses of IL-2 to NOD mice: toxicity and diabetes development.
135x101mm (300 x 300 DPI)

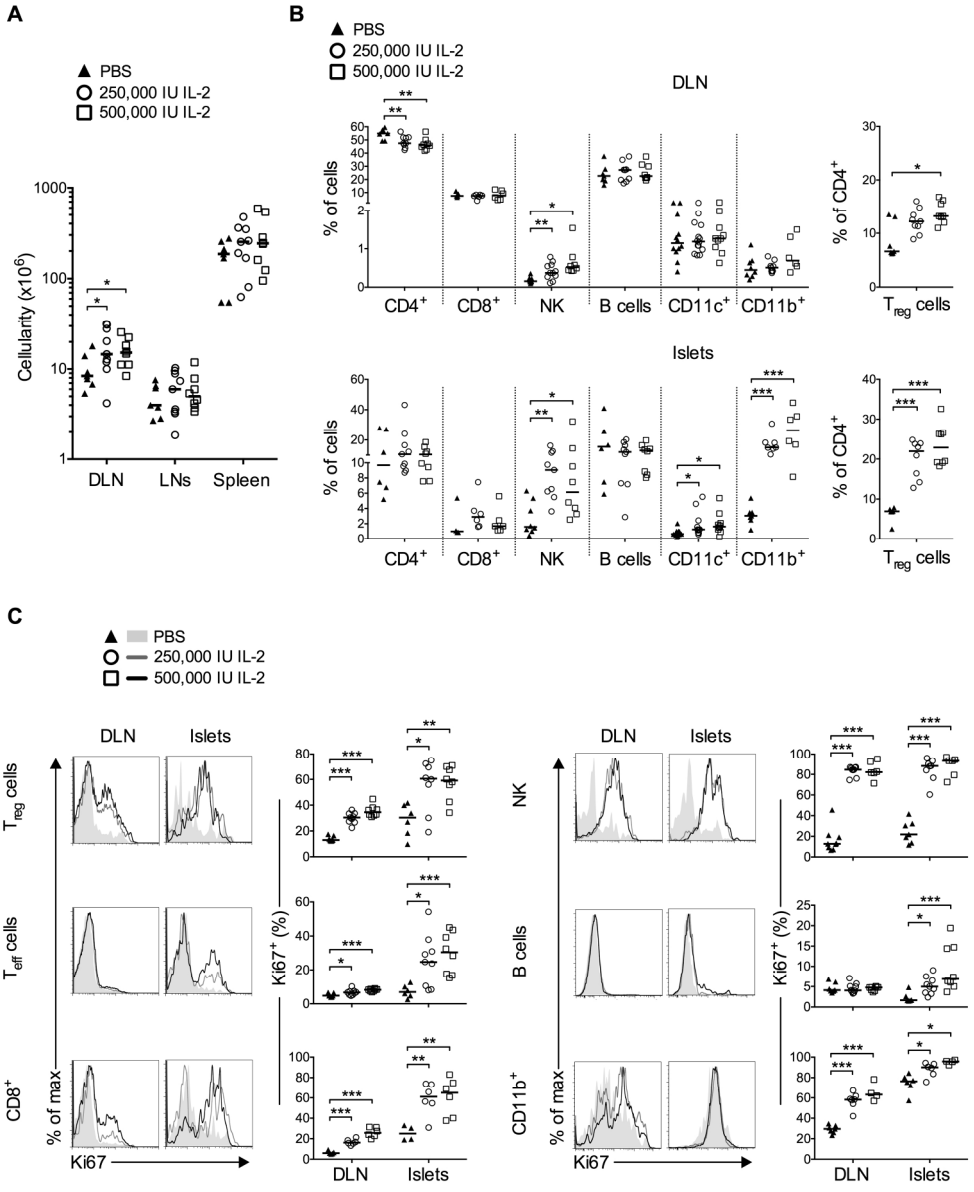

Figure 2. Administration of high doses of IL-2 to NOD mice: effects on immune cells.
220x269mm (300 x 300 DPI)

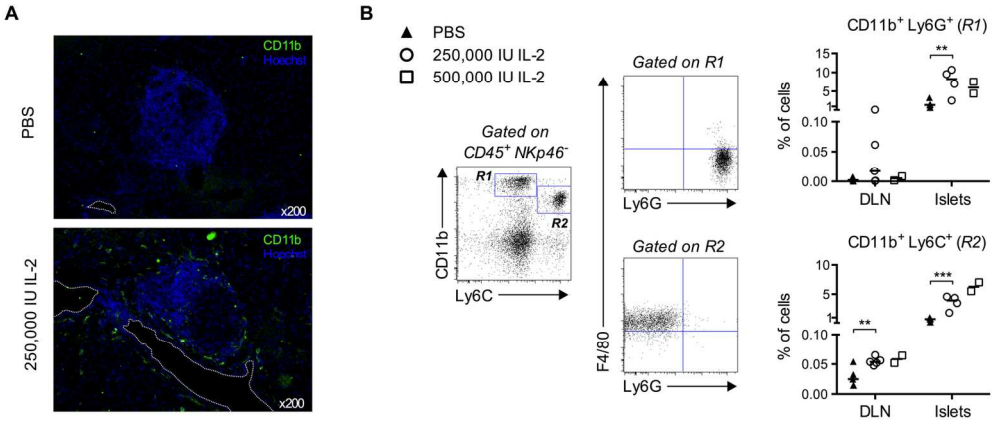

Figure 3. Administration of high doses of IL-2 to NOD mice: effects on myeloid cells.
78x34mm (600 x 600 DPI)

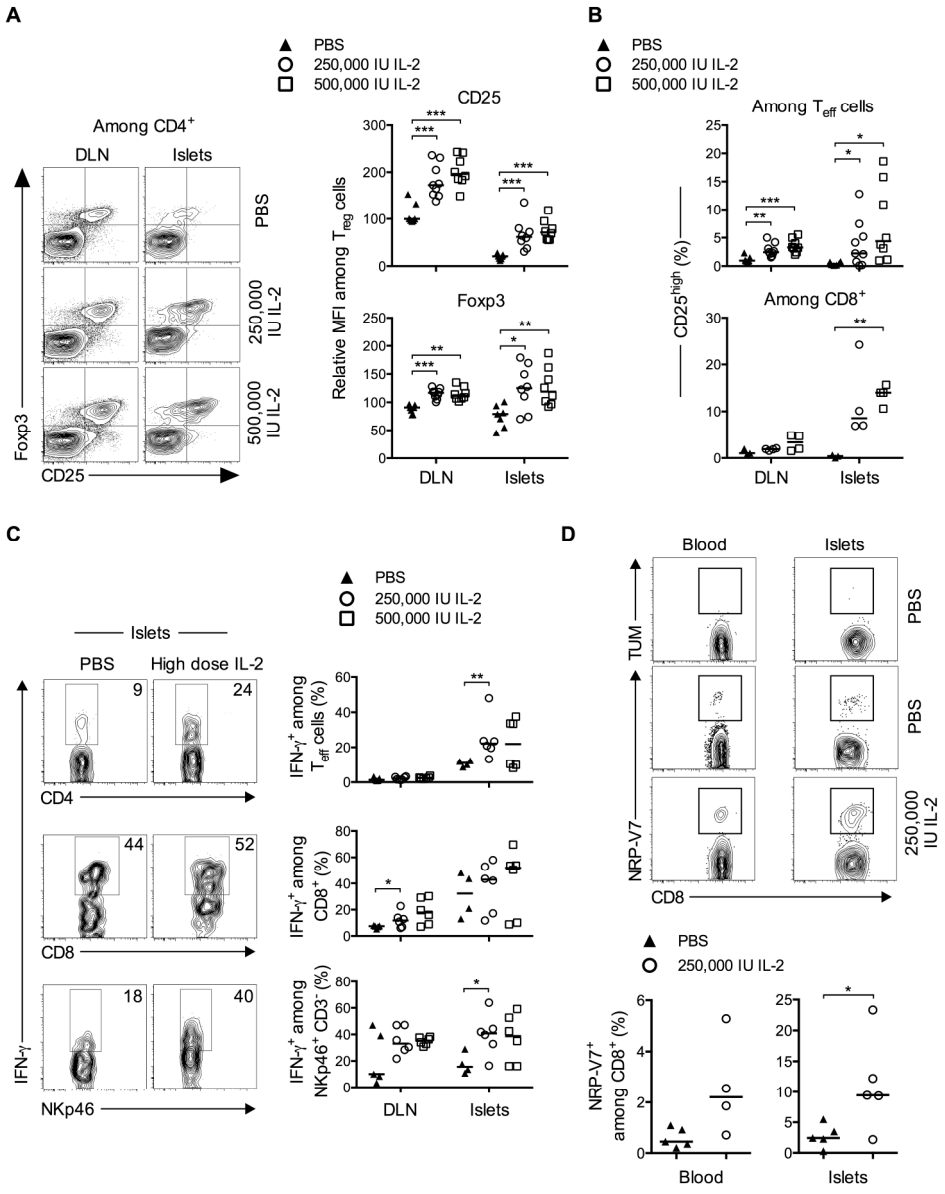

Figure 4. Administration of high doses of IL-2 to NOD mice: effects on cell activation and cytokine production.
226x284mm (300 x 300 DPI)

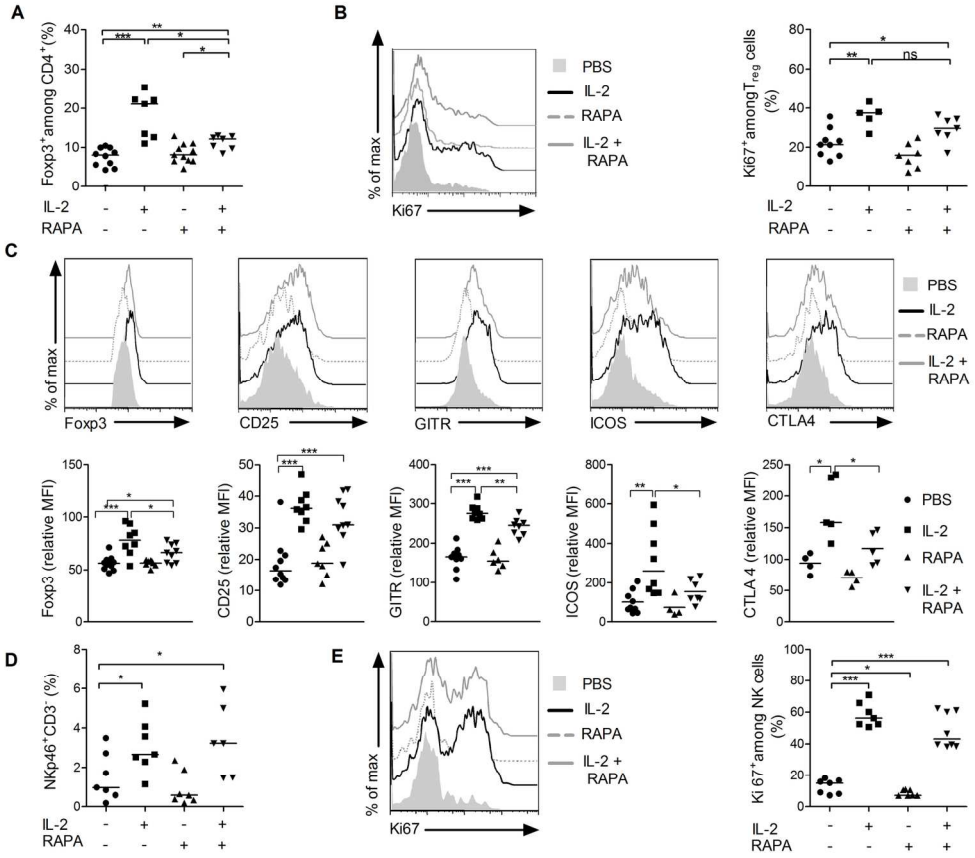

Figure 5. Effects of combined low-dose IL-2 and RAPA on immune cells.
158x139mm (300 x 300 DPI)

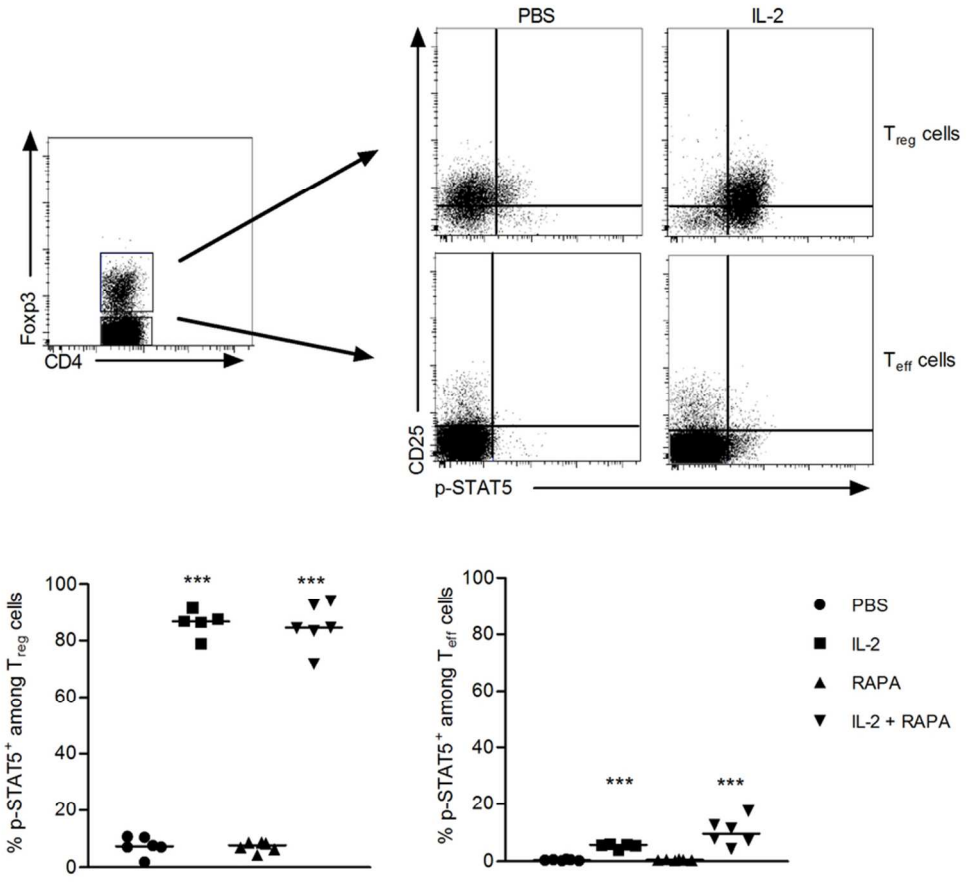

Figure 6. IL-2 and RAPA effects on STAT5 phosphorylation.
81x74mm (300 x 300 DPI)

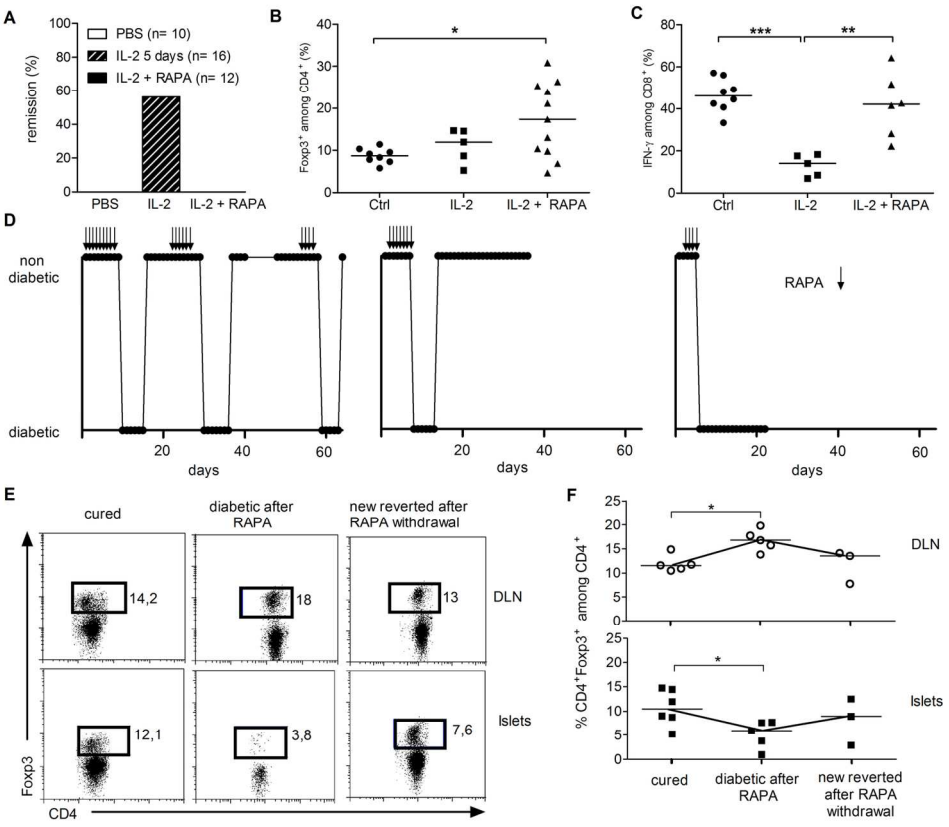

Figure 7: RAPA abrogates IL-2-induced tolerance.
152x130mm (300 x 300 DPI)

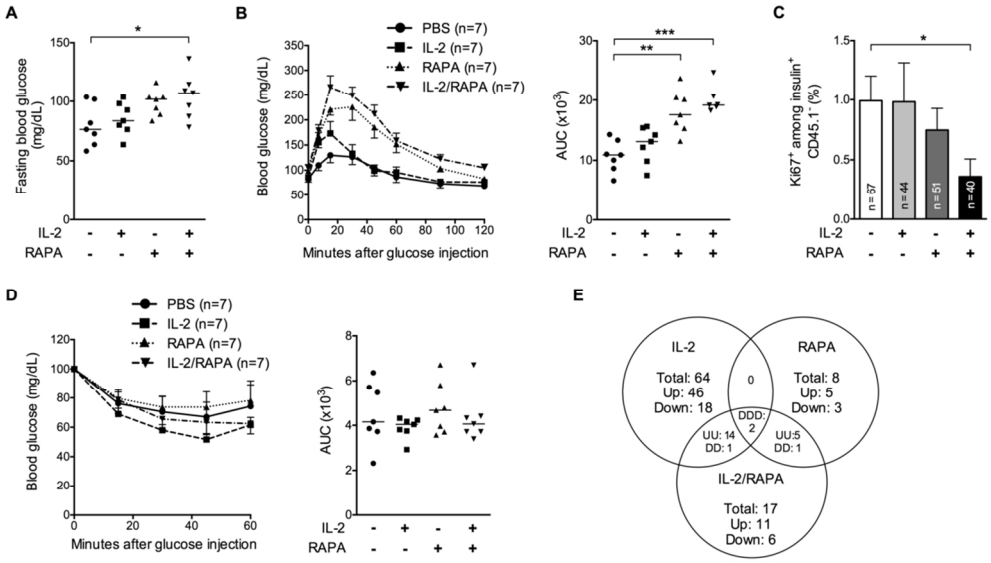

106x62mm (300 x 300 DPI)

Supplementary Figure 1

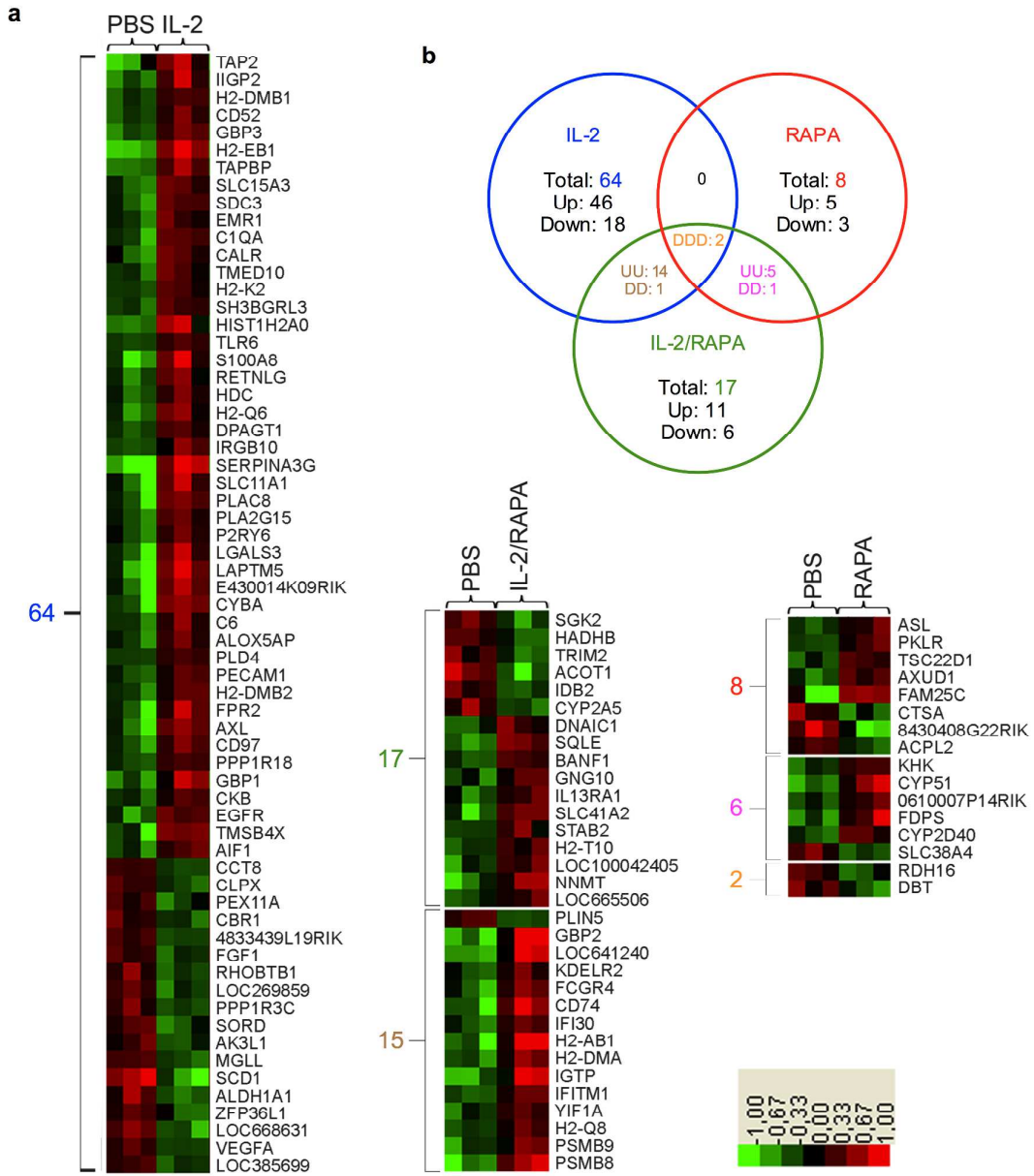

Supplementary Figure 1. RAPA alone or combined with IL-2 impacts on liver glucose metabolism: microarray analysis. Heat maps show the genes from the comparison of IL-2 vs PBS, IL-2/RAPA vs PBS and RAPA vs PBS lists, filtered at 1.5-fold change as depicted in the Venn diagram. The intensity of green and red colors indicates the degree of down or up-regulation, respectively.

Supplementary Table 1. RAPA alone or combined with IL-2 impacts on liver glucose metabolism: pathway analysis.

		Ingenuity Canonical Pathways	-log(p-value)	Ratio	Molecules
IL-2 ONLY	*Immune response*	Communication between Innate and Adaptive Immune Cells	3,26E00	7,53E-02	TLR2,IL1RN,TLR6,HLA-B,HLA-DRB1,CD86,HLA-F
		Complement System	1,75E00	9,09E-02	C8B,C1QA,C6
		IL-10 Signaling	1,52E00	5,56E-02	CCR5,BLVRA,IL1RN,CHUK
		IL-8 Signaling	2,33E00	4,69E-02	PLD4,VEGFA,RAC2,ARRB2,RHOG,CHUK,IQGAP1,FNBP1,EGFR
		Interferon Signaling	2,57E00	1,18E-01	OAS1,IFITM1,PSMB8,STAT1
		Lipid Antigen Presentation by CD1	1,37E00	9,09E-02	CALR,PDIA3
		NF-κB Signaling	1,63E00	4,12E-02	SIGIRR,TLR2,TGFBR2,IL1RN,TLR6,CHUK,EGFR
		Toll-like Receptor Signaling	2,59E00	8,77E-02	SIGIRR,TLR2,PPARA,TLR6,CHUK
	Metabolism	Lipoate Biosynthesis and Incorporation II	1,46E00	5E-01	LIAS
		PXR/RXR Activation	1,63E00	6,25E-02	PPARA,SCD,ALDH1A1,NR1I2
		Sorbitol Degradation I	1,76E00	1E00	SORD
		Sucrose Degradation V (Mammalian)	2,23E00	2,86E-01	ALDOB,GALM
		Superpathway of Citrulline Metabolism	1,62E00	1,43E-01	ASL,ARG1
RAPA ONLY	*Metabolism*	PI3K/AKT Signaling	1,83E00	2,96E-02	HSP90B1,NFKBIA,HSP90AB1,EIF4EBP1
		4-hydroxyproline Degradation I	1,81E00	5E-01	ALDH4A1
		Acetyl-CoA Biosynthesis I (Pyruvate Dehydrogenase Complex)	1,34E00	1,67E-01	DBT
		Arginine Degradation I (Arginase Pathway)	1,51E00	2,5E-01	ALDH4A1
		Ceramide Biosynthesis	1,34E00	1,67E-01	KDSR
		Citrulline-Nitric Oxide Cycle	1,42E00	2E-01	ASL
		NAD Biosynthesis from 2-amino-3-carboxymuconate Semialdehyde	1,34E00	1,67E-01	QPRT
		PPAR Signaling	1,48E00	3E-02	HSP90B1,NFKBIA,HSP90AB1
		PPARα/RXRα Activation	1,41E00	2,31E-02	ADCY9,HSP90B1,NFKBIA,HSP90AB1
		Proline Degradation	1,81E00	5E-01	ALDH4A1
		S-methyl-5-thio-α-D-ribose 1-phosphate Degradation	1,81E00	5E-01	APIP
IL-2/RAPA ONLY	*Metabolism*	1D-myo-inositol Hexakisphosphate Biosynthesis V (from Ins(1,3,4)P3)	1,47E00	3,33E-01	IPMK
		Acetone Degradation I (to Methylglyoxal)	1,46E00	7,69E-02	CYP2A13/CYP2A6,CYP51A1
		Epoxysqualene Biosynthesis	1,65E00	5E-01	SQLE
		Fatty Acid β-oxidation I	1,37E00	6,9E-02	HADHB,SLC27A2
		Isoleucine Degradation I	1,97E00	1,43E-01	HADHB,ACADSB
		L-serine Degradation	1,47E00	3,33E-01	SRR
		Stearate Biosynthesis I (Animals)	2,25E00	9,38E-02	SLC27A2,DBT,ELOVL1
		Superpathway of Geranylgeranyldiphosphate Biosynthesis I (via Mevalonate)	1,86E00	1,25E-01	FDPS,HADHB

		Tryptophan Degradation III (Eukaryotic)	1,76E00	1,11E-01	HADHB,HAAO
SHARED IL-2 AND IL-2/RAPA	*Immune response*	Antigen Presentation Pathway	6,78E00	1,75E-01	PSMB9,HLA-DMA,HLA-B,HLA-DMB,PSMB8,CD74,TAPBP
		CD28 Signaling in T Helper Cells	1,4E00	3,28E-02	CD3G,HLA-DMA,HLA-DMB,HLA-DQB1
		CTLA4 Signaling in Cytotoxic T Lymphocytes	1,72E00	4,21E-02	CD3G,HLA-DMA,HLA-DMB,HLA-DQB1
		Calcium-induced T Lymphocyte Apoptosis	3,3E00	8,2E-02	CD3G,HLA-DMA,HLA-DMB,HLA-DQB1,PRKD3
		Dendritic Cell Maturation	1,35E00	2,6E-02	HLA-DMA,HLA-B,HLA-DMB,HLA-DQB1,FCGR3A
		IL-4 Signaling	2,02E00	5,33E-02	HLA-DMA,IL13RA1,HLA-DMB,HLA-DQB1
		Nur77 Signaling in T Lymphocytes	2,58E00	7,02E-02	CD3G,HLA-DMA,HLA-DMB,HLA-DQB1
		OX40 Signaling Pathway	3,45E00	8,2E-02	CD3G,HLA-DMA,HLA-B,HLA-DMB,HLA-DQB1
		PKCθ Signaling in T Lymphocytes	1,4E00	3,15E-02	CD3G,HLA-DMA,HLA-DMB,HLA-DQB1
		Role of NFAT in Regulation of the Immune Response	1,92E00	3,23E-02	CD3G,HLA-DMA,HLA-DMB,HLA-DQB1,FCGR3A,GNG10
		T Helper Cell Differentiation	1,39E00	4,35E-02	HLA-DMA,HLA-DMB,HLA-DQB1
		iCOS-iCOSL Signaling in T Helper Cells	1,53E00	3,57E-02	CD3G,HLA-DMA,HLA-DMB,HLA-DQB1
	Metabolism	NAD biosynthesis II (from tryptophan)	2,04E00	1,54E-01	HAAO,QPRT
		Triacylglycerol Biosynthesis	3,3E00	1,21E-01	PPAPDC1B,AGPAT2,DBT,ELOVL1
		Valine Degradation I	2,99E00	1,67E-01	HADHB,ACADSB,DBT
SHARED RAPA AND IL-2/RAPA	*Metabolism*	Branched-chain α-keto acid Dehydrogenase Complex	1,35E00	2,5E-01	DBT
		Cholesterol Biosynthesis I	3,42E00	2,31E-01	SQLE,NSDHL,CYP51A1
		Cholesterol Biosynthesis II (via 24,25-dihydrolanosterol)	3,42E00	2,31E-01	SQLE,NSDHL,CYP51A1
		Cholesterol Biosynthesis III (via Desmosterol)	3,42E00	2,31E-01	SQLE,NSDHL,CYP51A1
		Geranylgeranyldiphosphate Biosynthesis	1,35E00	2,5E-01	FDPS
		Superpathway of Cholesterol Biosynthesis	4,93E00	1,85E-01	FDPS,SQLE,HADHB,NSDHL,CYP51A1
		Trans, trans-farnesyl Diphosphate Biosynthesis	1,35E00	2,5E-01	FDPS
		Triacylglycerol Biosynthesis	3,3E00	1,21E-01	PPAPDC1B,AGPAT2,DBT,ELOVL1
		Zymosterol Biosynthesis	2,73E00	3,33E-01	NSDHL,CYP51A1

Supplementary Table 1. RAPA alone or combined with IL-2 impacts on liver glucose metabolism: pathway analysis. The table shows the top canonical pathways, identified from the Ingenuity canonical pathways library that were most significant to the data sets filtered at 1.2-fold change (see figure 6). Relevant pathways were obtained according to the following 2 criteria: 1) Fischer's exact test was used to calculate a p-value determining the probability that the association between the genes in the dataset and the canonical pathway is explained by chance alone ("Log(Pvalue)"); and 2) A ratio of the number of genes from the data set that map to the pathway divided by the total number of genes that map to the canonical pathway is displayed ("Ratio"). "Molecules" show the genes from the data set included in the corresponding canonical pathway. Pathways were hand-cured and classified as immune (immune response) or metabolic (metabolism) pathways. Data are from one experiment with 3 biological replicates for each condition.

Supplementary Table 2. Outcome and mechanisms for all the different IL-2- and RAPA-based treatments attempted in the context of T1D prevention or reversal in the NOD mouse and humans.

Treatment/ Condition	***T1D prevention in NOD mice***	***T1D reversal in NOD mice***	***T1D prevention in human***	***T1D reversal in human***
High-dose IL-2 alone	Precipitates T1D, due to a shift from immune tolerance to destructive autoimmunity.	ND	ND	ND
Low-dose IL-2 alone	Prevents T1D in part by specifically boosting pancreatic T_{reg} cells (*ref 8 and 13*).	Reverts hyperglycemia, in part by specifically boosting pancreatic T_{reg} cells (*ref 9*)	ND	Completed. Awaiting results (*NCT01353833**)
RAPA alone	Prevents T1D (*ref 13,**a,b***)	No efficacy (*ref 14 and **b***)	ND	No negative effect (*ref 11*)
low-dose IL-2 + RAPA	Prevents T1D (*ref 13*)	No efficacy. RAPA counteracts IL-2 benefic effects on Tregs but not on NK cells.	Transient β-cell dysfunction. Increase in Tregs, eosinophils and NK cells (*NCT00525889**)	

		Induces glucose intolerance.	

ND: not done

* ClinicalTrials.gov Identifier

a- Rapamycin prevents the onset of insulin-dependent diabetes mellitus (IDDM) in NOD mice. Baeder WL, Sredy J, Sehgal SN, Chang JY, Adams LM. Clin Exp Immunol. 1992 Aug;89(2):174-8.

b- Combination therapy with low dose sirolimus and tacrolimus is synergistic in preventing spontaneous and recurrent autoimmune diabetes in non-obese diabetic mice. Shapiro AM, Suarez-Pinzon WL, Power R, Rabinovitch A. Diabetologia. 2002 Feb;45(2):224-30.

SUPPLEMENTARY DATA

Supplementary Table 1. RAPA alone or combined with IL-2 impacts on liver glucose metabolism: pathway analysis. The table shows the top canonical pathways, identified from the Ingenuity canonical pathways library that were most significant to the data sets filtered at 1.2-fold change (see figure 6). Relevant pathways were obtained according to the following 2 criteria: 1) Fischer's exact test was used to calculate a p-value determining the probability that the association between the genes in the dataset and the canonical pathway is explained by chance alone ("Log(Pvalue)"); and 2) A ratio of the number of genes from the data set that map to the pathway divided by the total number of genes that map to the canonical pathway is displayed ("Ratio"). "Molecules" show the genes from the data set included in the corresponding canonical pathway. Pathways were hand-cured and classified as immune (immune response) or metabolic (metabolism) pathways. Data are from one experiment with 3 biological replicates for each condition.

		Ingenuity Canonical Pathways	-log(p-value)	Ratio	Molecules
IL-2 ONLY	*Immune response*	Communication between Innate and Adaptive Immune Cells	3,26E00	7,53E-02	TLR2,IL1RN,TLR6,HLA-B,HLA-DRB1,CD86,HLA-F
		Complement System	1,75E00	9,09E-02	C8B,C1QA,C6
		IL-10 Signaling	1,52E00	5,56E-02	CCR5,BLVRA,IL1RN,CHUK
		IL-8 Signaling	2,33E00	4,69E-02	PLD4,VEGFA,RAC2,ARRB2,RHOG,CHUK,IQGAP1,FNBP1,EGFR
		Interferon Signaling	2,57E00	1,18E-01	OAS1,IFITM1,PSMB8,STAT1
		Lipid Antigen Presentation by CD1	1,37E00	9,09E-02	CALR,PDIA3
		NF-κB Signaling	1,63E00	4,12E-02	SIGIRR,TLR2,TGFBR2,IL1RN,TLR6,CHUK,EGFR
		Toll-like Receptor Signaling	2,59E00	8,77E-02	SIGIRR,TLR2,PPARA,TLR6,CHUK
	Metabolism	Lipoate Biosynthesis and Incorporation II	1,46E00	5E-01	LIAS
		PXR/RXR Activation	1,63E00	6,25E-02	PPARA,SCD,ALDH1A1,NR1I2
		Sorbitol Degradation I	1,76E00	1E00	SORD
		Sucrose Degradation V (Mammalian)	2,23E00	2,86E-01	ALDOB,GALM
		Superpathway of Citrulline Metabolism	1,62E00	1,43E-01	ASL,ARG1
RAPA ONLY	*Metabolism*	PI3K/AKT Signaling	1,83E00	2,96E-02	HSP90B1,NFKBIA,HSP90AB1,EIF4EBP1
		4-hydroxyproline Degradation I	1,81E00	5E-01	ALDH4A1
		Acetyl-CoA Biosynthesis I (Pyruvate Dehydrogenase Complex)	1,34E00	1,67E-01	DBT
		Arginine Degradation I (Arginase Pathway)	1,51E00	2,5E-01	ALDH4A1
		Ceramide Biosynthesis	1,34E00	1,67E-01	KDSR
		Citrulline-Nitric Oxide Cycle	1,42E00	2E-01	ASL
		NAD Biosynthesis from 2-amino-3-carboxymuconate Semialdehyde	1,34E00	1,67E-01	QPRT
		PPAR Signaling	1,48E00	3E-02	HSP90B1,NFKBIA,HSP90AB1
		PPARα/RXRα Activation	1,41E00	2,31E-02	ADCY9,HSP90B1,NFKBIA,HSP90AB1
		Proline Degradation	1,81E00	5E-01	ALDH4A1
		S-methyl-5-thio-α-D-ribose 1-phosphate Degradation	1,81E00	5E-01	APIP
IL-2/RAPA	*Metabolis*	1D-myo-inositol Hexakisphosphate Biosynthesis V (from	1,47E00	3,33E-01	IPMK

SUPPLEMENTARY DATA

ONLY	*m*	Ins(1,3,4)P3)			
		Acetone Degradation I (to Methylglyoxal)	1,46E00	7,69E-02	CYP2A13/CYP2A6,CYP51A1
		Epoxysqualene Biosynthesis	1,65E00	5E-01	SQLE
		Fatty Acid β-oxidation I	1,37E00	6,9E-02	HADHB,SLC27A2
		Isoleucine Degradation I	1,97E00	1,43E-01	HADHB,ACADSB
		L-serine Degradation	1,47E00	3,33E-01	SRR
		Stearate Biosynthesis I (Animals)	2,25E00	9,38E-02	SLC27A2,DBT,ELOVL1
		Superpathway of Geranylgeranyldiphosphate Biosynthesis I (via Mevalonate)	1,86E00	1,25E-01	FDPS,HADHB
		Tryptophan Degradation III (Eukaryotic)	1,76E00	1,11E-01	HADHB,HAAO
SHARED IL-2 AND IL-2/RAPA	*Immune response*	Antigen Presentation Pathway	6,78E00	1,75E-01	PSMB9,HLA-DMA,HLA-B,HLA-DMB,PSMB8,CD74,TAPBP
		CD28 Signaling in T Helper Cells	1,4E00	3,28E-02	CD3G,HLA-DMA,HLA-DMB,HLA-DQB1
		CTLA4 Signaling in Cytotoxic T Lymphocytes	1,72E00	4,21E-02	CD3G,HLA-DMA,HLA-DMB,HLA-DQB1
		Calcium-induced T Lymphocyte Apoptosis	3,3E00	8,2E-02	CD3G,HLA-DMA,HLA-DMB,HLA-DQB1,PRKD3
		Dendritic Cell Maturation	1,35E00	2,6E-02	HLA-DMA,HLA-B,HLA-DMB,HLA-DQB1,FCGR3A
		IL-4 Signaling	2,02E00	5,33E-02	HLA-DMA,IL13RA1,HLA-DMB,HLA-DQB1
		Nur77 Signaling in T Lymphocytes	2,58E00	7,02E-02	CD3G,HLA-DMA,HLA-DMB,HLA-DQB1
		OX40 Signaling Pathway	3,45E00	8,2E-02	CD3G,HLA-DMA,HLA-B,HLA-DMB,HLA-DQB1
		PKCθ Signaling in T Lymphocytes	1,4E00	3,15E-02	CD3G,HLA-DMA,HLA-DMB,HLA-DQB1
		Role of NFAT in Regulation of the Immune Response	1,92E00	3,23E-02	CD3G,HLA-DMA,HLA-DMB,HLA-DQB1,FCGR3A,GNG10
		T Helper Cell Differentiation	1,39E00	4,35E-02	HLA-DMA,HLA-DMB,HLA-DQB1
		iCOS-iCOSL Signaling in T Helper Cells	1,53E00	3,57E-02	CD3G,HLA-DMA,HLA-DMB,HLA-DQB1
	Metabolism	NAD biosynthesis II (from tryptophan)	2,04E00	1,54E-01	HAAO,QPRT
		Triacylglycerol Biosynthesis	3,3E00	1,21E-01	PPAPDC1B,AGPAT2,DBT,ELOVL1
		Valine Degradation I	2,99E00	1,67E-01	HADHB,ACADSB,DBT
SHARED RAPA AND IL-2/RAPA	*Metabolism*	Branched-chain α-keto acid Dehydrogenase Complex	1,35E00	2,5E-01	DBT
		Cholesterol Biosynthesis I	3,42E00	2,31E-01	SQLE,NSDHL,CYP51A1
		Cholesterol Biosynthesis II (via 24,25-dihydrolanosterol)	3,42E00	2,31E-01	SQLE,NSDHL,CYP51A1
		Cholesterol Biosynthesis III (via Desmosterol)	3,42E00	2,31E-01	SQLE,NSDHL,CYP51A1
		Geranylgeranyldiphosphate Biosynthesis	1,35E00	2,5E-01	FDPS
		Superpathway of Cholesterol Biosynthesis	4,93E00	1,85E-01	FDPS,SQLE,HADHB,NSDHL,CYP51A1
		Trans, trans-farnesyl Diphosphate Biosynthesis	1,35E00	2,5E-01	FDPS
		Triacylglycerol Biosynthesis	3,3E00	1,21E-01	PPAPDC1B,AGPAT2,DBT,ELOVL1
		Zymosterol Biosynthesis	2,73E00	3,33E-01	NSDHL,CYP51A1

SUPPLEMENTARY DATA

Supplementary Table 2. Outcome and mechanisms for all the different IL-2- and RAPA-based treatments attempted in the context of T1D prevention or reversal in the NOD mouse and humans.

Treatment/ Condition	***T1D prevention in NOD mice***	***T1D reversal in NOD mice***	***T1D prevention in human***	***T1D reversal in human***
High-dose IL-2 alone	Precipitates T1D, due to a shift from immune tolerance to destructive autoimmunity.	ND	ND	ND
Low-dose IL-2 alone	Prevents T1D in part by specifically boosting pancreatic T_{reg} cells (*ref 8 and 13*).	Reverts hyperglycemia, in part by specifically boosting pancreatic T_{reg} cells (*ref 9*)	ND	Completed. Awaiting results (*NCT01353833**)
RAPA alone	Prevents T1D (*ref 13,**a,b***)	No efficacy (*ref 14 and **b***)	ND	No negative effect (*ref 11*)
low-dose IL-2 + RAPA	Prevents T1D (*ref 13*)	No efficacy. RAPA counteracts IL-2 benefic effects on Tregs but not on NK cells. Induces glucose intolerance.	Transient β-cell dysfunction. Increase in Tregs, eosinophils and NK cells (*NCT00525889**)	

ND: not done

* ClinicalTrials.gov Identifier

a- Rapamycin prevents the onset of insulin-dependent diabetes mellitus (IDDM) in NOD mice. Baeder WL, Sredy J, Sehgal SN, Chang JY, Adams LM. Clin Exp Immunol. 1992 Aug;89(2):174-8.

b- Combination therapy with low dose sirolimus and tacrolimus is synergistic in preventing spontaneous and recurrent autoimmune diabetes in non-obese diabetic mice. Shapiro AM, Suarez-Pinzon WL, Power R, Rabinovitch A. Diabetologia. 2002 Feb;45(2):224-30.

SUPPLEMENTARY DATA

Supplementary Figure 1. RAPA alone or combined with IL-2 impacts on liver glucose metabolism: microarray analysis. Heat maps show the genes from the comparison of IL-2 vs PBS, IL-2/RAPA vs PBS and RAPA vs PBS lists, filtered at 1.5-fold change as depicted in the Venn diagram. The intensity of green and red colors indicates the degree of down or up-regulation, respectively.